

# Head-to-head Comparison of Qualitative Radiologist Assessment With Automated Quantitative Computed Tomography Analysis for Bronchiolitis Obliterans Syndrome After Hematopoietic Cell Transplantation

Husham Sharifi, MD, MS,\* Zachary D. Guenther, MD,†  
Ann N.C. Leung, MD,† Laura Johnston, MD,‡ Yu K. Lai, MD,\*  
Joe L. Hsu, MD, MPH,\* and H. Henry Guo, MD, PhD†

**Purpose:** Computed tomography (CT) findings of bronchiolitis obliterans syndrome (BOS) can be nonspecific and variable. This study aims to measure the incremental value of automated quantitative lung CT analysis to clinical CT interpretation. A head-to-head comparison of quantitative CT lung density analysis by parametric response mapping (PRM) with qualitative radiologist performance in BOS diagnosis was performed.

**Materials and Methods:** Inspiratory and end-expiratory CTs of 65 patients referred to a post-bone marrow transplant lung graft-versus-host-disease clinic were reviewed by 3 thoracic radiologists for the presence of mosaic attenuation, centrilobular opacities, airways dilation, and bronchial wall thickening. Radiologists' majority consensus diagnosis of BOS was compared with automated PRM air trapping quantification and to the gold-standard diagnosis of BOS as per National Institutes of Health (NIH) consensus criteria.

**Results:** Using a previously established threshold of 28% air trapping on PRM, the diagnostic performance for BOS was as follows: sensitivity 56% and specificity 94% (area under the receiver operator curve [AUC]=0.75). Radiologist review of inspiratory CT images alone resulted in a sensitivity of 80% and a specificity of 69% (AUC=0.74). When radiologists assessed both inspiratory and end-expiratory CT images in combination, the sensitivity was 92% and the specificity was 59% (AUC=0.75). The highest performance was observed when the quantitative PRM report was reviewed alongside inspiratory and end-expiratory CT images, with a sensitivity of 92% and a specificity of 73% (AUC=0.83).

**Conclusions:** In the CT diagnosis of BOS, qualitative expert radiologist interpretation was noninferior to quantitative PRM. The highest level of diagnostic performance was achieved by the combination of quantitative PRM measurements with qualitative image feature assessments.

**Key Words:** bronchiolitis obliterans syndrome, quantitative computed tomography, air trapping, mosaic attenuation, hematopoietic stem cell transplant

(*J Thorac Imaging* 2021;00:000–000)

From the \*Department of Medicine, Division of Pulmonary, Allergy, and Critical Care Medicine; †Department of Radiology, Stanford University School of Medicine; and ‡Department of Medicine, Division of Blood and Marrow Transplantation, Stanford University School of Medicine, Stanford, CA.

H.S. and Z.D.G. are co-first authors.

The authors declare no conflict of interest.

Correspondence to: H. Henry Guo, MD, PhD, Department of Radiology, Stanford University School of Medicine, Grant Building S074A, 300 Pasteur Drive, Stanford CA 94305-5236 (e-mail: henryguo@stanford.edu).

Supplemental Digital Content is available for this article. Direct URL citations appear in the printed text and are provided in the HTML and PDF versions of this article on the journal's website, [www.thoracicimaging.com](http://www.thoracicimaging.com).

Copyright © 2021 Wolters Kluwer Health, Inc. All rights reserved.  
DOI: 10.1097/RTI.0000000000000595

Translation of quantitative imaging biomarkers into clinical chest computed tomography (CT) promises to advance thoracic imaging.<sup>1</sup> Extensive developmental efforts have been applied to quantitative lung CT analysis, with applications across a range of diffuse lung diseases: emphysema, asthma, fibrosing interstitial lung diseases, COVID-19 lung infection burden,<sup>2</sup> and bronchiolitis obliterans syndrome (BOS).<sup>3–8</sup> These analyses have been successfully applied to broad research populations (eg, COPDGene),<sup>9,10</sup> but there are relatively limited data on the impact of incorporating quantitative lung CT biomarkers into clinical practice. In the context of diagnosing BOS, we assessed the performance of computer-aided automated quantitative CT metrics against the qualitative approach to lung CT interpretation that is the current standard of care.

BOS, a form of chronic graft-versus-host-disease (cGVHD), is the most serious long-term noninfectious pulmonary complication after hematopoietic stem cell transplant (HCT).<sup>11</sup> BOS typically occurs within 12 to 24 months after transplant<sup>12</sup> and manifests as new-onset fixed airflow obstruction. The gold-standard clinical diagnosis is based on National Institutes of Health (NIH) criteria of obstruction by pulmonary function tests and imaging in the absence of infection (see Supplemental Data File for detailed criteria, Supplemental Digital Content 1, <http://links.lww.com/JTI/A190>).<sup>13,14</sup> The reported incidence of BOS is variable but likely underestimated due to the difficulty in making the diagnosis in the presence of potential concurrent pulmonary infections, organizing pneumonia, and cGVHD manifesting as sclerodermatous skin of the thorax (truncal sclerosis).<sup>15</sup> A large single-center retrospective cohort demonstrated that the prevalence of BOS according to the NIH consensus definition is 5.5% for all allogeneic HCT recipients and 14% in those with extrapulmonary manifestations of cGVHD.<sup>16</sup>

Qualitative findings of BOS on CT have been reported to consist of air trapping, centrilobular opacities, airways dilation, and bronchial wall thickening.<sup>11,17–19</sup> Although there have been efforts to quantify the degree of airways dilation in this population,<sup>20</sup> the threshold at which these features are considered positive can be subjective. In contrast, parametric response mapping (PRM) is an automated software algorithm that classifies lung parenchymal disease based on a voxel-by-voxel comparison of lung attenuation changes between inspiration and expiration. It has shown promise as an imaging biomarker for obstructive lung diseases<sup>21</sup> and in the diagnosis of post-HCT BOS.<sup>8</sup> Whether lung CT densitometry can offer improved identification of BOS compared with radiologist interpretation based on qualitative features is unknown.

Using a well-characterized cohort of allogeneic HCT patients followed in our medical center's lung graft-versus-host-disease (GVHD) clinic, we therefore studied the impact of

PRM and qualitative interpretation for BOS diagnosis by radiologist interpretation of CTs and by the published air trapping threshold for BOS (ie, 28%).<sup>8</sup> These were compared to the gold-standard clinician diagnosis by NIH criteria.<sup>13</sup> A subset of these data with differing diagnostic adjudication and disease classification was used in a previous machine learning study by our group<sup>22</sup> (see Supplemental Data File for details, Supplemental Digital Content 1, <http://links.lww.com/JTI/A190>). The association of pertinent imaging findings was also analyzed with respect to PRM metrics, thus offering an integrated approach for quantitative and qualitative assessments to enhance clinician and radiologist diagnosis of BOS.

## MATERIALS AND METHODS

### Study Population

For this study, we used a well-characterized database of PRM CT scans in patients followed in our medical center's lung GVHD clinic. Post-HCT patients were enrolled in the current study if they had a documented complaint of dyspnea and underwent chest CT with PRM air trapping quantification within the data collection period from June 2015 to June 2018. Of the resulting 79 eligible patients, 14 individuals were excluded due to loss to follow-up ( $n=1$ ); lack of pre-HCT ( $n=1$ ) or follow-up ( $n=2$ ) pulmonary function tests; or technically suboptimal CT scans ( $n=10$ , most frequently due to inadequate breathholds and respiratory motion). Nine of the remaining 65 patients contributed >1 scan, resulting in a total of 76 PRM scans that were analyzed individually in a blinded manner.

The gold-standard diagnosis was established as isolated BOS (ie, without coexisting lung disease) by consensus agreement of 2 board-certified pulmonologists (H.S., J.L.H.) and a board-certified hematologist (L.J.) following NIH criteria (25 patients).<sup>13</sup> All fields of the CT PRM analysis were recorded, namely, percentage air trapping, percentage emphysema-like lung, percentage normal lung, expiratory lung volume, and inspiratory lung volume.

### CT Technique and Radiology Assessment

Noncontrast volumetric thoracic CT scanning at full inspiration (total lung capacity) and end expiration (residual volume) was performed (Siemens Force; Siemens Medical Systems, Erlangen, Germany; GE Discovery CT750 HD, GE Healthcare, Chicago, IL). Expiratory images were contiguous, without skipped images. Scans performed with the Siemens scanner had a 515×512 reconstruction matrix, 192×0.6 mm collimation, 120 kV, rotation time 0.25 seconds, pitch 1, and CareDose4 at QRM125. Images were reconstructed at 1 mm axial slice thickness with a sharp reconstruction algorithm (filter Br54) for visual assessment and a neutral reconstruction algorithm (filter Bf32) at 0.7 mm increment for PRM analysis. Scans performed with the GE scanner had a 515×512 reconstruction matrix, 64×0.625 mm collimation, 120 kV, rotation time 0.5 seconds, pitch 1.375, and SmartMA at NI52. Images were reconstructed at 1.25 mm axial slice thickness with a bone kernel for visual assessment and a standard kernel at 0.8 mm increment for PRM analysis. PRM was acquired using lung segmentation and image registration of paired inspiratory and expiratory images performed by a Food and Drug Administration (FDA)-approved software algorithm (Lung Density Analysis, Imbio, Minneapolis, MN, [https://imbio-web-public.s3.amazonaws.com/Lung+Density+Analysis/Versions/3.0.0/USA/DES-7197+Imbio\\_CT\\_LDA\\_3.0\\_SW\\_Manual\\_US.pdf](https://imbio-web-public.s3.amazonaws.com/Lung+Density+Analysis/Versions/3.0.0/USA/DES-7197+Imbio_CT_LDA_3.0_SW_Manual_US.pdf)). Voxels were classified based on ranges of Hounsfield

units following a standardized protocol (Supplemental Data File, Supplemental Digital Content 1, <http://links.lww.com/JTI/A190>).

CT scans were independently reviewed and scored by 3 thoracic radiologists (Z.D.G., 5 y of experience; H.H.G., 12 y of experience; A.N.C.L., 28 y of experience) who were blinded to patient identification and clinical information. Radiologists were able to adjust window/level settings manually. To simulate clinical interpretation and assess the relative contributions of the inspiratory phase, expiratory phase, and CT imaging features to BOS diagnosis, radiologists were provided with progressively greater information in 3 sequential stages (Fig. 1). First, axial inspiratory images were assessed for presence or absence of airways dilation, bronchial wall thickening, centrilobular opacities, and mosaic attenuation, as per published imaging criteria for BOS.<sup>11,17</sup> The extent of the mosaic attenuation was scored semiquantitatively as none, low (less than one third of lung parenchyma), or high (greater than or equal to one third of lung parenchyma) (see Supplemental Data File for details, Supplemental Digital Content 1, <http://links.lww.com/JTI/A190>) using previously established methods.<sup>23,24</sup> In the inspiratory phase, the radiologist diagnosed the absence or presence of BOS and their corresponding degree of confidence on a scale from 1 to 3, the latter representing the highest confidence. At the second stage, the radiologist reviewed the axial end-expiratory images and inspiratory images of the same patient to assess the degree of mosaic attenuation and again provided a binary diagnosis of BOS and corresponding confidence level. At the third and final stage in the same session, the radiologist reviewed the PRM report that quantified percentage air trapping and again provided a binary BOS diagnosis with confidence level. In a separate analysis, the presence of BOS was determined by PRM report alone using previously established criteria of >28% persistent low-density area.<sup>8</sup>

### Statistical Analysis

Consensus values of binary CT attributes (mosaic attenuation, airways dilation, bronchial wall thickening, centrilobular nodules) and BOS diagnosis were rounded to the nearest integer. Given the binary nature of these parameters, the consensus value represented either perfect consensus or a 2-versus-1 tiebreak (ie, a two third majority vote). Consensus data for extent of mosaic attenuation and confidence levels were assessed by taking the mean for each variable entered by the 3 radiologists and rounding to the nearest integer when appropriate. Metrics for CT chest attributes were analyzed using the  $\chi^2$  test.  $P$ -values <0.05 were considered significant. For the diagnosis of consensus radiologist reads, a 95% confidence interval was assessed for each area under the curve (AUC). Unadjusted univariate logistic regression was applied to CT scan attributes separately to assess association with pure BOS as the response variable. Multivariate logistic regression assigned multiple CT scan attributes as covariates to perform risk adjustment. Odds ratios were calculated from the beta coefficients of covariates. All statistical analyses were carried out in R, version 3.6.1 ([www.r-project.org](http://www.r-project.org)) with the caret package for analytics of radiologist performance.

## RESULTS

### Study Cohort

Sixty-five patients formed the analytic cohort. Given that 9 patients received >1 CT chest, a total of 76 PRM CT scans

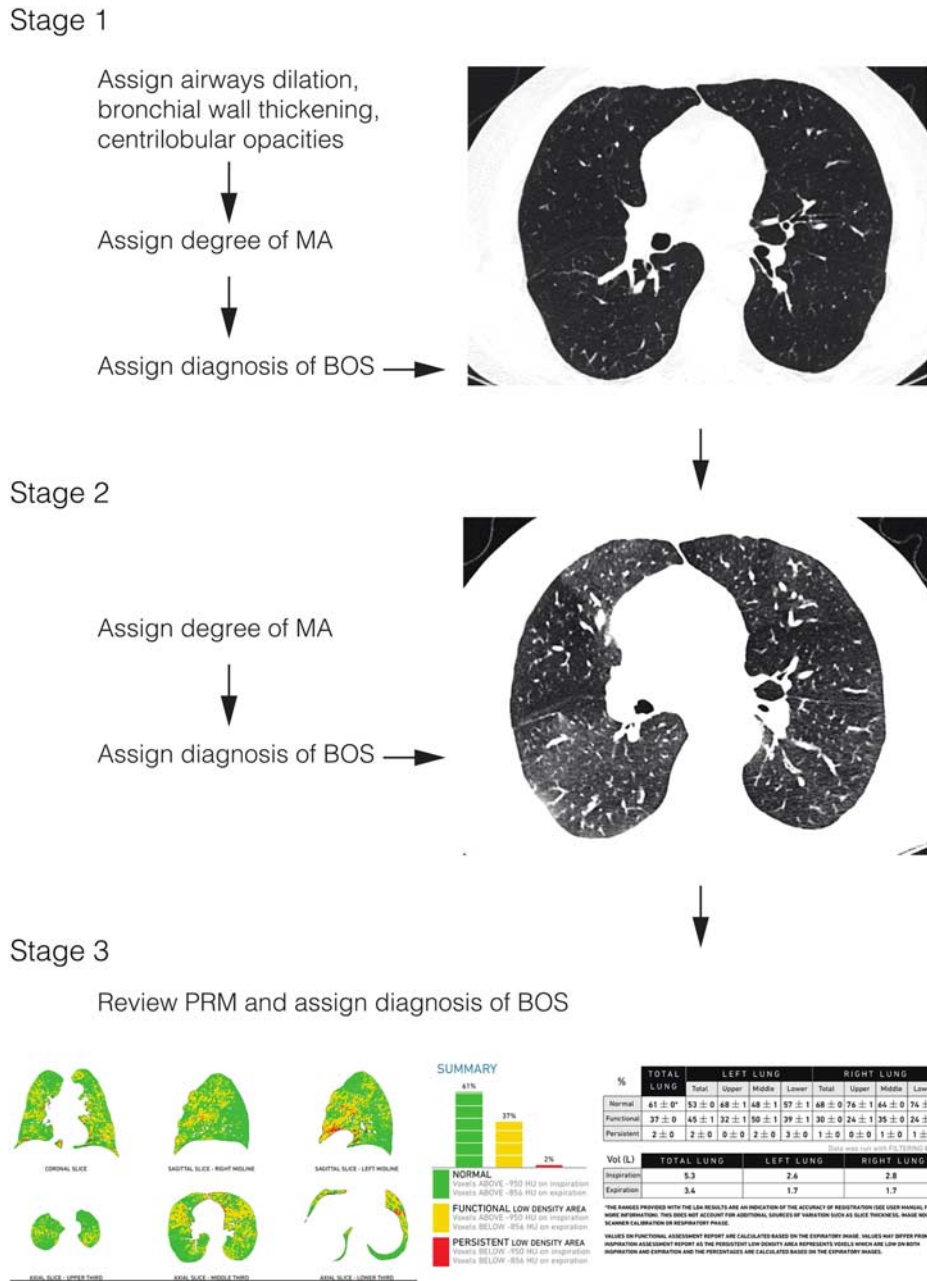


**FIGURE 1.** Example of 3-stage step-wise interpretation of chest CT for BOS diagnosis. Stage 1: CT images obtained in the inspiratory phase reviewed for features reported in BOS: airways dilation, bronchial wall thickening, centrilobular opacities, and mosaic attenuation (MA). Severity of MA is scored as none, low, or high, and the diagnosis of BOS with confidence level is made (see the Materials and methods section). In the case shown, airways dilation and centrilobular opacities (visible on other slices) were present, bronchial wall thickening was absent, MA was scored as low, and the scan was judged to be positive for BOS with low confidence. Stage 2: CT images obtained at the end-expiratory phase were then provided at the same session, with repeat scoring of MA severity and BOS diagnosis. In the case shown, MA scored increased to high, and the diagnosis was positive for BOS with moderate confidence. Stage 3: Automated, lung voxel density-based PRM air trapping quantification report was then made available to the radiologist at the same session. In the case shown, PRM calculated 37% air trapping (see Supplemental Data File for the software calculation method, Supplemental Digital Content 1, <http://links.lww.com/JTI/A190>). The patient was diagnosed with BOS with high confidence. [full color online](#)

were analyzed to assess each CT chest as an independent diagnostic challenge. Twenty-five scans were from 22 patients with BOS without concomitant lung disease. The mean age was 52 years, with 20% of patients having a history of

obstructive lung disease before HCT (Table 1). Ninety percent of patients had cGVHD of at least 1 organ, diagnosed at a median of 26 months after HCT. Over a 19-month median length of follow-up, the overall mortality was 16.9%.

**TABLE 1.** Cohort Demographics\*

	n (%)
No. PRM CT scans analyzed	76
No. patients	65
Age, mean (SD)	52.0 (12.5)
Male	37 (56.9)
History of previous obstructive lung disease	13 (19.6)
History of smoking	20 (30.8)
cGVHD	60 (92.3)
Pulmonary complications after HCT†	
BOS	25 (32.9)
OP	8 (10.5)
TS	13 (17.1)
BOS+OP	4 (5.3)
BOS+TS	4 (5.3)
Infection	3 (3.9)
Fibrosis	3 (3.9)
None	16 (21.1)
Mortality	11 (16.9)

\*Demographics are presented for 65 patients who underwent a total of 76 CT chest scans.

†Represents the number of complications in the cohort of 76 CT chest scans. For example, 25 scans were from patients diagnosed with BOS by NIH criteria. OP indicates organizing pneumonia; TS, truncl sclerosis.

In assessing the association of imaging attributes with the gold-standard diagnosis, mosaic attenuation and airways dilation revealed the strongest correlation (Table 2). Univariate logistic regression showed that these 2 features maintained statistical significance with large odds ratios (Table 3). To control for correlation of imaging attributes, we performed multivariate regression and found that only the association for mosaic attenuation with BOS maintained statistical significance (odds ratio = 6.0, 95% confidence interval: 1.9-20.1,  $P = 0.002$ ).

In the context of mosaic attenuation being associated with BOS diagnosis by correlation and regression analysis, we sought to assess the sensitivity and specificity of quantitative air trapping on PRM as a solitary diagnostic marker (Fig. 2). The specificity of BOS diagnosis was 90.5% at 16% air trapping and 95.2% at 21% air trapping. In contrast, the sensitivity of BOS diagnosis increased only with low air trapping levels (eg, 86% sensitivity at 8% air trapping).

To explore the correlation of visual severity of mosaic attenuation with percent air trapping by PRM, we analyzed quantitative air trapping percentage against consensus mosaic attenuation. For mosaic attenuation evaluated on inspiratory images (Fig. 3A), the mean air trapping percentage differed significantly when comparing studies with scores of “none” to “low” (8.6% vs. 25.1% air trapping, respectively,  $P < 0.00001$ )

**TABLE 2.** Association of Lung CT Attributes Versus Ground Truth Diagnosis of BOS\*

	$\chi^2$ Value	P
Mosaic attenuation (expiratory)	14.3	0.0002
Airways dilation	8.0	0.0046
Mosaic attenuation (inspiratory)	5.7	0.0169
Bronchial wall thickening	3.2	0.0729
Centrilobular nodules	1.2	0.2723

\*N = 76.

Presence of lung CT attribute was determined by consensus radiologist assessment, as described in the Materials and methods section.

**TABLE 3.** Association of Lung CT Attributes as Assessed by Radiologists With a Diagnosis of BOS\*

	Odds Ratio	95% Confidence Interval
Expiratory mosaic attenuation	8.3	2.9-25.9
Airways dilation	5.9	1.9-22.5
Bronchial wall thickening	2.8	1.0-8.0
Centrilobular nodules	2.2	0.7-7.4
Mosaic attenuation after risk adjustment	6.0	1.9-20.1

\*N = 76.

Presence of lung CT attribute was determined by consensus radiologist assessment, as described in the Materials and methods section. The first 4 rows show the results of univariate regression. Mosaic attenuation in the fifth row is reported after risk adjustment by airways dilation, bronchial wall thickening, and centrilobular nodules.

or “none” to “high” mosaic attenuation (8.6% vs. 40.3%, respectively,  $P = 0.003$ ). For end-expiratory mosaic attenuation (Fig. 3B), mean air trapping differed when comparing studies with scores of “none” to “low” (7.5% vs. 17.5% air trapping, respectively,  $P = 0.001$ ) or “none” to “high” mosaic attenuation (7.5% vs. 27.4% air trapping, respectively,  $P = 0.0003$ ). No other pairings achieved statistical significance.

We explored the correlation of mosaic attenuation with quantitative air trapping among the 25 scans from patients with BOS and found the following groups: presence of mosaic attenuation with high air trapping percentage (16/25); presence of mosaic attenuation with low air trapping percentage (6/25); and absence of mosaic attenuation with high air trapping percentage (1/25) (Figs. 4A–C). Figure 4D shows a patient without BOS, with CT demonstrating lack of mosaic attenuation and low quantitative air trapping.

We sought to understand how radiologist diagnosis based on qualitative imaging features compared to the previously published air trapping threshold of 28% for BOS diagnosis<sup>8</sup> (Table 4, Fig. 5). For the inspiratory phase, we found a diagnostic accuracy of 72%, a sensitivity of 80%, a specificity of 69%, and an AUC of 0.74. Adding the expiratory phase, we found an accuracy of 70%, a sensitivity of

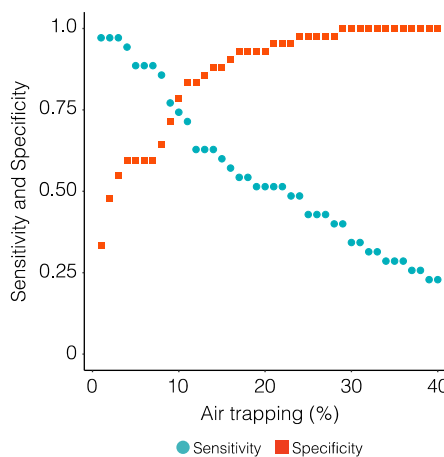


**FIGURE 2.** Sensitivity and specificity of increasing quantified PRM air trapping percentage with respect to ground truth diagnosis of pure BOS. full color online

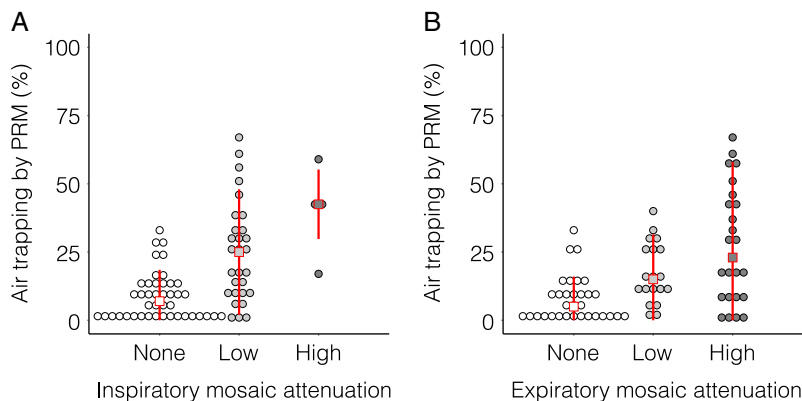


**FIGURE 3.** Air trapping percentage quantified by automated PRM versus categories for the percentage of lung that show mosaic attenuation as assessed by radiologists. **A,** The assessment of inspiratory CT images. **B,** The assessment of expiratory CT images. Categories for mosaic attenuation are by consensus assessment of radiologists, as defined in Materials and methods section. Each dot represents 1 CT chest. The red square shows the median and the vertical red line shows the interquartile range. [full color online](#)

92%, a specificity of 59%, and an AUC of 0.75. Subsequent addition of quantitative PRM output yielded an accuracy of 79%, a sensitivity of 92%, a specificity of 73%, and an AUC of 0.83. In contrast, the air trapping threshold of 28% by PRM, when used alone, achieved an accuracy of 82%, a sensitivity of 56%, a specificity of 94%, and an AUC of 0.75.

To understand the performance characteristics of radiologist interpretation, we studied BOS diagnosis by radiologist confidence in CT interpretation. High confidence labels were applied to 7 of 76 scans (9.1%) with only inspiratory phase images, and 6 of these 7 scans were diagnosed correctly as BOS (86% accuracy). High confidence labels were applied to 7 of 76 scans (9.1%) in the combined analysis of both inspiratory and expiratory phase images, and all of these 7 scans were diagnosed correctly as BOS. The addition of PRM quantitative air trapping percentage increased radiologists' interpretative confidence, and high confidence labels were applied to 26 of 76 scans (24%) when radiologists reviewed inspiratory and expiratory images along with PRM output, and 25 of these 26 scans were diagnosed correctly as BOS (96% accuracy). The following associations of BOS diagnosis with imaging features were found in the group of 26 high-confidence CTs: mosaic attenuation in the expiratory phase ( $\chi^2 = 11.1, P = 0.0008$ ), airways dilation ( $\chi^2 = 7.8, P = 0.005$ ), bronchial wall thickening ( $\chi^2 = 5.7, P = 0.017$ ), and centrilobular nodularity ( $\chi^2 = 4.0, P = 0.05$ ). In contrast to feature assessment with all scans, in which only mosaic attenuation and airways dilation achieved statistical significance, radiologists achieved significance for all imaging features when their confidence in BOS diagnosis was high.

**DISCUSSION**

In this study, we demonstrated that the combination of radiologist assessment and quantitative lung density analysis resulted in improved diagnostic accuracy for BOS when compared to radiologist's qualitative interpretation or to air trapping quantification by PRM alone. These findings parallel those of other studies that report improved performance when radiologist interpretation is assisted by output from automated algorithms, such as in distinguishing COVID-19 lung infection from other pneumonias.<sup>25</sup>

In assessing the relative importance of CT imaging attributes in BOS, we found by correlation and regression analysis that mosaic attenuation had a consistent association with the clinical diagnosis of BOS. Although quantitative air trapping has been explored in previous studies as a surrogate biomarker for mosaic attenuation,<sup>8,26</sup> our study showed that sensitivity and specificity varied widely according to the degree of air trapping percentage (Fig. 2). Based on these analyses, we sought to understand how combining the characteristics of mosaic attenuation and quantitative air trapping improved diagnostic accuracy for BOS and found that the 2 parameters sometimes diverged (Figs. 3, 4). This suggested that the presence or absence of mosaic attenuation is useful in distinguishing explicit cases of BOS, but that the extent of mosaic attenuation may be limited in diagnosing early BOS or identifying differing severities of BOS, as has been also described by Konen et al<sup>23</sup> in patients with BOS after lung transplant.

The apparent discrepancy between CT appearance of lack of mosaic attenuation and high air trapping quantification by PRM seen in 1 of 25 scans from BOS patients (Fig. 4C) may arise from obliterative bronchiolitis being extensive and diffuse, with decreased heterogenous appearance of mosaic attenuation on CT despite geographically widespread air trapping in this case. In the opposite instance of present mosaic attenuation but low PRM air trapping percentage in BOS (6/25 scans) (Fig. 4B), concomitant ground-glass may accentuate the appearance of mosaic attenuation, but decrease the calculated PRM air trapping percentage due to overall increased lung density. Greater heterogeneity of small airways obstruction may also account for more prominent appearance of mosaic attenuation in some cases.

Assessment of the various visual and quantitative biomarkers across inspiratory and expiratory phases revealed stepwise improvements in diagnostic performance for BOS. Addition of end-expiratory CT to inspiratory imaging alone improved the sensitivity but decreased the specificity, similar to what has previously been demonstrated in postlung transplant BOS.<sup>27</sup> Addition of PRM air trapping quantification to assessment of inspiratory and expiratory imaging improved specificity and maintained the gains in sensitivity, with minimal additional radiologist interpretation time incurred, estimated to be approximately or <1 minute. Our study contrasts with a previous study by Galban et al,<sup>8</sup> which used a quantitative air trapping threshold of 28% for the diagnosis of BOS. Applying this threshold to our cohort

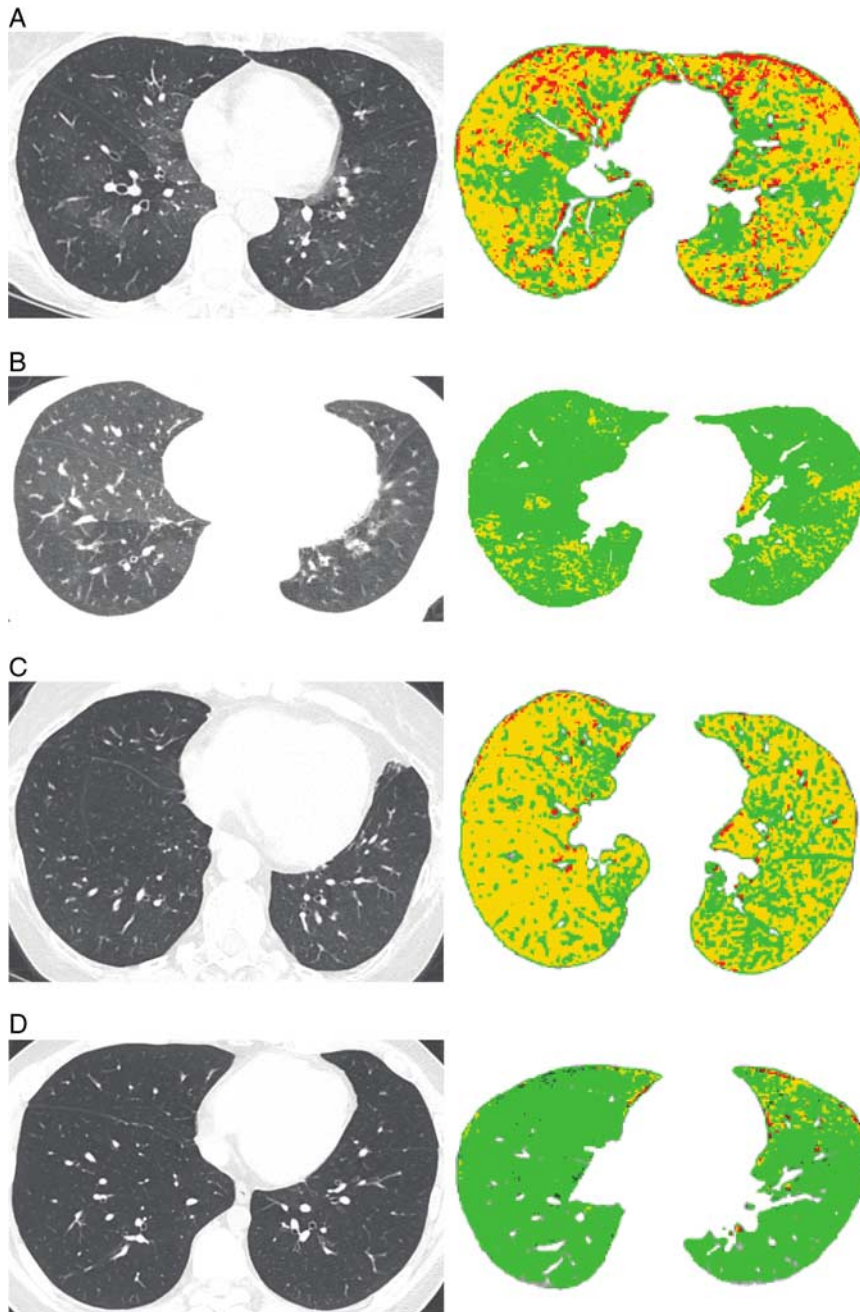


**FIGURE 4.** Example cases of high and low mosaic attenuation on expiratory axial cuts of lung CT scans with high and low air trapping as quantified by PRM. A–C, Patients who were diagnosed clinically with BOS. A, High mosaic attenuation and high PRM quantified air trapping at 44%. B, High mosaic attenuation and relatively low quantified air trapping of 14%. C, A patient with apparently low mosaic attenuation, despite high quantified air trapping of 59%. D, A patient with the clinical diagnosis of not having BOS and illustrates low mosaic attenuation and low air trapping of 2%. full color online

yielded a specificity of 94% and a sensitivity of 56%, with important differences in study design. Galban and colleagues compared BOS to infection. In the context of assessing pure BOS only, we compared against patients with any lung disease—organizing pneumonia, fibrosis, infection—as well as patients without lung disease. PRM percentage air trapping quantification as a solitary marker is limited in its

ability to capture the full physiology of these other conditions. Our analysis illustrates that the optimal air trapping threshold depends on the clinical context.

Our study is subject to several limitations. Patients referred for quantitative PRM analysis were assessed at a dedicated lung GVHD clinic, which necessarily makes the presence of BOS more likely. Second, to decrease the effects

**TABLE 4.** Diagnostic Performance for Consensus Radiologist Interpretation for the Diagnosis of BOS\*

	Inspiratory Phase	Inspiratory+Expiratory Phase	Inspiratory+Expiratory Phase+PRM	Air Trapping $\geq 28\%$
Sensitivity	0.80	0.92	0.92	0.56
Specificity	0.69	0.59	0.73	0.94
PPV	0.56	0.52	0.62	0.82
NPV	0.88	0.94	0.95	0.81
Accuracy	0.72	0.70	0.79	0.82
AUC (95% CI)	0.74 (0.64-0.85)	0.75 (0.67-0.84)	0.83 (0.74-0.91)	0.75 (0.65-0.86)

\*N = 76.

CI indicates confidence interval; NPV, negative predictive value; PPV, positive predictive value.

of interobserver variability in this study, we used a majority consensus approach from a panel of radiologists from a single center with high HCT volume. This approach may limit generalizability from routine clinical CT interpretation and from nontertiary care environments. Hence, a potential advantage of threshold-based automated quantitative lung CT is to enable more standardized interpretative results across a variety of practice settings.<sup>1,3</sup> Third, this study is limited to 3 thoracic radiologists. We sought to mitigate this limitation by involving radiologists with a spectrum of experience levels and assessing statistical association by multiple approaches, including the following: (1) correlation; (2) regression analysis with and without risk adjustment; (3) sensitivity and specificity of imaging biomarkers; (4) comparison of imaging features such as mosaic attenuation with PRM air trapping quantification; and (5) stratification of scans by diagnostic confidence of reads. Analytic results consistently demonstrated that mosaic attenuation was associated with a diagnosis of BOS and that there were subgroups of BOS patients in whom mosaic attenuation and quantitative air trapping diverge. Nonetheless, future studies will benefit from a larger number of radiologists in multiple centers. Fourth, the diagnosis of BOS relies on criteria that include the absence of active lung infection, given that infection can cause transient airflow obstruction. Infection in our study was excluded in all cases to the extent possible by bronchoscopy with bronchoalveolar lavage and

microbiological testing, as well as clinical follow-up. Finally, this study focused on patients with the gold-standard diagnosis of bronchiolitis obliterans. Patients with coexistent conditions such as infection, organizing pneumonia, and truncal sclerosis, with superimposed imaging findings that could confound qualitative and quantitative measurements, were excluded from analysis. The coexistence of these conditions with BOS highlights the challenges of chest CT interpretation in a complex patient population and suggests the need for a multidisciplinary approach in patient management of lung GVHD.

In conclusion, this study stratifies the relative importance of a set of qualitative CT imaging features for BOS and demonstrates that automated PRM air trapping quantification plays an adjunctive role in the analysis of CT chest scans for patients with BOS. The use of imaging features, coupled with PRM quantitative CT analysis, can assist radiologists with improved diagnosis of lung cGVHD.

**ACKNOWLEDGMENTS**

The authors thank our patients in the lung GVHD clinic of our medical center.

**REFERENCES**

1. Kay FU, Oz OK, Abbara S, et al. Translation of quantitative imaging biomarkers into clinical chest CT. *Radiographics*. 2019; 39:957–976.
2. Huang L, Han R, Ai T, et al. Serial quantitative chest CT assessment of COVID-19: deep-learning approach. *Radiol Cardiothorac Imaging*. 2020;2:e200075.
3. Silva M, Milanese G, Seletti V, et al. Pulmonary quantitative CT imaging in focal and diffuse disease: current research and clinical applications. *Br J Radiol*. 2018;91:20170644.
4. Bankier AA, De Maertelaer V, Keyzer C, et al. Pulmonary emphysema: Subjective visual grading versus objective quantification with macroscopic morphometry and thin-section CT densitometry. *Radiology*. 1999;211:851–858.
5. Trivedi A, Hall C, Hoffman EA, et al. Using imaging as a biomarker for asthma. *J Allergy Clin Immunol*. 2017;139:1–10.
6. Bartholmai BJ, Raghunath S, Karwoski RA, et al. Quantitative computed tomography imaging of interstitial lung diseases. *J Thorac Imaging*. 2013;28:298–307.
7. Galbán CJ, Han MK, Boes JL, et al. Computed tomography-based biomarker provides unique signature for diagnosis of COPD phenotypes and disease progression. *Nat Med*. 2012;18:1711–1715.
8. Galban CJ, Boes JL, Bule M, et al. Parametric response mapping as an indicator of bronchiolitis obliterans syndrome after hematopoietic stem cell transplantation. *Biol Blood Marrow Transplant*. 2014;20:1592–1598.
9. Han MK, Kazerooni EA, Lynch DA, et al. Chronic obstructive pulmonary disease exacerbations in the COPDGene Study: associated radiologic phenotypes. *Radiology*. 2011;261:274–282.
10. Han MLK, Tayob N, Murray S, et al. Association between emphysema and chronic obstructive pulmonary disease outcomes in

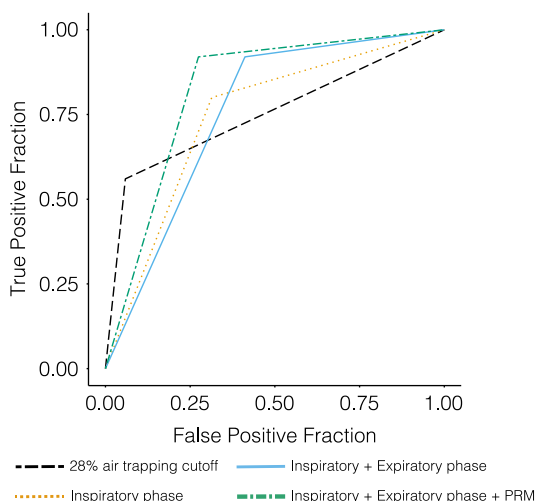


**FIGURE 5.** Receiver operating characteristic curves for diagnosing pure BOS from 28% air trapping on PRM and from radiologist assessment of the PRM inspiratory phase, expiratory phase, and quantitative output of PRM software processing.

- the COPDGene and SPIROMICS cohorts: a post hoc analysis of two clinical trials. *Am J Respir Crit Care Med*. 2018;198:265–267.
11. Gunn MLD, Godwin JD, Kanne JP, et al. High-resolution CT findings of bronchiolitis obliterans syndrome after hematopoietic stem cell transplantation. *J Thorac Imaging*. 2008;23:244–250.
  12. Williams KM. How I treat bronchiolitis obliterans syndrome after hematopoietic stem cell transplantation. *Blood*. 2017;129:448–455.
  13. Jagasia MH, Greinix HT, Arora M, et al. National Institutes of Health Consensus Development Project on Criteria for Clinical Trials in Chronic Graft-versus-Host Disease: I. The 2014 Diagnosis and Staging Working Group Report. *Biol Blood Marrow Transplant*. 2015;21:389.e1–401.e1.
  14. Shulman HM, Cardona DM, Greenson JK, et al. NIH Consensus Development Project on Criteria for Clinical Trials in Chronic Graft-versus-Host Disease: II. The 2014 Pathology Working Group Report. *Biol Blood Marrow Transplant*. 2015;21:589–603.
  15. Bergeron A, Cheng G-S. Bronchiolitis obliterans syndrome and other late pulmonary complications after allogeneic hematopoietic stem cell transplantation. *Clin Chest Med*. 2017;38:607–621.
  16. Au BKC, Au MA, Chien JW. Bronchiolitis obliterans syndrome epidemiology after allogeneic hematopoietic cell transplantation. *Biol Blood Marrow Transplant*. 2011;17:1072–1078.
  17. Padley SPG, Adler BD, Hansell DM, et al. Bronchiolitis obliterans: high resolution CT findings and correlation with pulmonary function tests. *Clin Radiol*. 1993;47:236–240.
  18. Sargent MA, Cairns RA, Murdoch MJ, et al. Obstructive lung disease in children after allogeneic bone marrow transplantation: evaluation with high-resolution CT. *AJR Am J Roentgenol*. 1995;164:693–696.
  19. Jung JI, Jung WS, Hahn ST, et al. Bronchiolitis obliterans after allogeneic bone marrow transplantation: HRCT findings. *Korean J Radiol*. 2004;5:107.
  20. Gazourian L, Coronata AMF, Rogers AJ, et al. Airway dilation in bronchiolitis obliterans after allogeneic hematopoietic stem cell transplantation. *Respir Med*. 2013;107:276–283.
  21. Boes JL, Hoff BA, Bule M, et al. Parametric response mapping monitors temporal changes on lung CT scans in the Subpopulations and Intermediate Outcome Measures in COPD Study (SPIROMICS). *Acad Radiol*. 2015;22:186–194.
  22. Sharifi H, Lai YK, Guo H, et al. Machine learning algorithms to differentiate among pulmonary complications after hematopoietic cell transplant. *Chest*. 2020;158:1090–1103.
  23. Konen E, Gutierrez C, Chaparro C, et al. Bronchiolitis obliterans syndrome in lung transplant recipients: can thin-section CT findings predict disease before its clinical appearance? *Radiology*. 2004;231:467–473.
  24. Miller WT, Chatzkel J, Hewitt MG. Expiratory air trapping on thoracic computed tomography: a diagnostic subclassification. *Ann Am Thorac Soc*. 2014;11:874–881.
  25. Bai HX, Hsieh B, Xiong Z, et al. Performance of radiologists in differentiating COVID-19 from viral pneumonia on chest CT. *Radiology*. 2020;296:E46–E54.
  26. Lynch DA, Al-Qaisi MA. Quantitative computed tomography in chronic obstructive pulmonary disease. *J Thorac Imaging*. 2013;28:284–290.
  27. Siegel MJ, Bhalla S, Gutierrez FR, et al. Post-lung transplantation bronchiolitis obliterans syndrome: usefulness of expiratory thin-section CT for diagnosis. *Radiology*. 2001;220:455–462.